ОБЪЕДИНЕННЫЙ
ИНСТИТУТ
ЯДЕРНЫХ
ИССЛЕДОВАНИЙ
Дубна



E2 - 6706

V.S.Barashenkov, K.K.Gudima, F.G.Gereghi,
A.S.Iljinov, V.D.Toneev

# MONTE CARLO CALCULATIONS OF REACTIONS INDUCED BY HIGH ENERGY PARTICLES AND RELATIVISTIC NUCLEI

1972

ЛАБОРАТОРИЯ ТЕОРЕТИЧЕСКОЙ ФИЗИКИ

E2 - 6706

V.S.Barashenkov, K.K.Gudima, F.G.Gereghi,
A.S.Iljinov, V.D.Toneev

# MONTE CARLO CALCULATIONS OF REACTIONS INDUCED BY HIGH ENERGY PARTICLES AND RELATIVISTIC NUCLEI

(Talk given at the Conference in the USA, June, 1972).

## Summary

As a comparative study of calculations by various authours reveals, the intranuclear cascade model which involves evaporation (or more fast decay) of the residual nucleus agrees well with experiment, for energies higher than several dozens of MeV. In the high-energy region ($T \gtrsim 0.5$-$1$ GeV for light nuclei, and $T \gtrsim 3$-$5$ GeV for heavy nuclei) it is necessary to take account of decreasing of matter density of the target-nucleus due to knocking out of a large number of target constituents by the cascade particles. Interactions of the produced resonances $\rho$, $\omega$, $N^*$ and so on with the nuclear nucleons contribute rather little to the cascade development. At the present time the least known and the most difficult for calculations remain just the high-energy fission of heavy nuclei and the phenomena occuring at the relativistic nuclei collisions. If the fission of the excited residual nuclei is calculated by means of statistical methods and the fission barriers are defined from the phenomenological approach which describes the mean experimental values, then one can obtain a rather good agreement with known experimental data on the cross sections of fission, on multiplicity, on angular and energy distribution of accompanying particles. Calculations for intranuclear cascades initiated by the light incident nuclei $d$, $t$, $^3He$, $\alpha$ agree with experiment, as well. However the experimental information available here for comparison is still poor. The latter concerns very much interactions with heavier bombarding nuclei C, N, O, etc. The cascade-evaporation model which we have developed, makes such calculations possible and gives a rather good agreement with experiment. Some observed disagreements are explained by the fact that the model provides a somewhat overestimated number of intranuclear collisions. For the further evolution of this model one needs first of all the more accurate experimental data.

1. A lot of calculations performed by means of the Monte-Carlo cascade-evaporation model for inelastic pion- and nucleon-nuclear interactions demonstrate that this model describes well average characteristics of interactions at all energies higher than several dozens of MeV (see refs.[1-4], where further bibliography is given). To what extent the calculations agree with experiment, are determined mainly by the chosen variant of the model, i.e. by its "grain structure". Our calculations take account of diffusivity of the nuclear matter density and of intranuclear potential and exploit the statistical simulation of characteristics of each act of inelastic and elastic intractions of particles inside a nucleus, with accurate fulfilment of the energy-momentum conservation law (see ref.[4] for details). Figs. 1-3 illustrate the agreement with experiment on the example of such "delicate" quantity as double differential cross-section $d^2\sigma/d\Omega\, dT$ *.

It should be recognized that the agreement

---

*Here and in the following $T$ is the kinetic energy of incident particles or nucleus (per nucleon) in lab.system, $T$ - is the kinetic energy of secondaries in the same system.

is quite satisfactory not only in the form of distribution but in the absolute value as well. Deviations from experiment become even less noticeable if instead of $d^2\sigma / d\Omega\, dT$ the integral angular and energy distributions $d\sigma/d\Omega$, $d\sigma/dT$ or average multiplicity $\bar{n}$ are considered.

In the energy region where it is still possible to neglect the meson production, a detailed comparative study for different variants of the cascade model has been carried out, following the suggestion of G.Friedlander. This has been made for those variants which are used in Dubna, Brookhaven, Columbia University and Oak-Ridge[5]. This analysis shows that aside from some disagreements in details of distributions, especially noticeable for energies of the excited nuclei which remain after a cascade, the final distributions of the reaction products turn out to be surprisingly similar for all three confronted variants of the model (see figs.4-6).

Among many investigated up-to-now characteristics, we can now indicate two points only where, as we think really essential disagreements with present cascade-evaporation model take place. Firstly, this is the yield of the low-energy particles: neutrons with $T \lesssim 2$ MeV and protons with an energy near the Coulomb barrier (see Fig. 7). No reasonable variation of parameters can cancel the above disagreement which obviously occurs due to neglecting a contribution of nonequilibrium processes. Second important discrepancy between experiment and theory is connected with the double charge-exchange reactions of the pions. Seven to ten-fold

divergence between calculated and measured cross-sections for this reaction is so high, that one cannot hope to remove it by any simple fitting of parameters. Obviously this evidences that the double charge-exchange phenomenon proceeds via some other mechanism and not by mere sequence of the elastic intranuclear collisions with charge exchange.

Thus more accurate experimental investigation of low-energy component of particles emitted by a nucleus and of the various properties of the charge-exchange (double and single) processes seems to us to be very important.

2. All considered variants of the conventional cascade-evaporation model assume usually that intranuclear cascade can be looked upon as successive independent binary collisions. At high energies this approximation will undoubtedly not be valid because the number of particles in the cascade shower becomes so large that there occurs the effective "trailing" of nucleus due to the knocking out of target nucleons by the cascade particles /3,6,7/. In other words, every nuclear nucleon having suffered a collision with the cascade particle, should be also treated further as a cascade particle. This results in local changes of density of the target-nucleus. In particular, the observed "saturation" of mean number of grey and black prongs in the photoemulsion stars at $T \gtrsim 3$-5 GeV (Fig. 8) are explained just by the above phenomena. This is the direct result of "saturation" of the intranuclear cascade with respect to the recoil nucleons and excitation energy of the residual nucleus. An account of

this effect allows one to predict also that the parameters which characterize the mass distributions of residual nuclei at energies of the order of several GeV should tend to the saturation. This really is confirmed by the radiochemical measurements of yield for different isotopes in the middle of Mendeleev Table. One can point out at a number of other important phenomena caused by the "trailing" effect[7]. The most essential is an account of this effect in the case of calculations for nucleus-nucleus interactions (see below).

The cascade model involving the "trailing" effect treats a nucleus as composed by separate nucleons instead of using the continuous distribution of the nuclear matter in conventional cascade model. Center positions of these nucleons are sampled by the Monte-Carlo method from the appropriate distribution $\rho(r)$ taken from experiment on the electron scattering. Here it is required that the distances between the nucleon centers would not be smaller than $2r_c$ where $r_c = 0.4 \cdot 10^{-13}$ cm is the kern radius of a nucleon[3,6,7]. Coordinates of all nucleons of the target-nucleus are stored by a computer.

As calculations reveal, a density decrease occurs already at energies $T \geq 0.5$-1 GeV in light nuclei, and the heavy nuclei at $T \geq 3$-5 GeV.

3. Aside from the local change of nuclear density, at high energies one more effect can be indicated which usually is not included in the cascade calculations but, generally speaking, can contribute significantly. This effect is that

at energies higher than several GeV the $\rho$-, $\omega$-, $N^*$, etc., resonon production occurs in the $\pi$-N and N-N interactions. Then these resonances if having the life-time large enough can be involved in the intranuclear cascade.

In fact, for the resonons with widths $\Gamma \simeq (100\text{-}200)$ MeV the life-time in the proper coordinate system $\tau \simeq (0.3\text{-}0.7)10^{-23}$ sec. If now one takes into consideration the relativistic dilation of time and the Pauli principle (the latter is especially essential for low-energy baryonic resonons), then a resonon can have time to interact with the nuclear nucleon before its decay. From the kinematical point of view this is the same as with the nuclear nucleon several "stuck together" particles interact simultaneously. As a result there should decrease the number of intranuclear collisions. This, in turn, will cause a decrease of the number of slow secondaries (mainly, the recoil nucleons) and the excitation energy of a nucleus as well.

Since the information on the resonon production cross sections and especially on the resonon-nucleon interactions is very poor, only an estimate of the resonon contribution to the intranuclear cascade can be found at the present time. We have confined ourselves to such assumptions on interactions involving resonons under which the resonon contribution would be maximal[8]. We have supposed that in <u>each</u> inelastic $\pi$-N and N-N collision inside the nucleus just one resonon is produced what is justified rather well by the present experimental data on probabilities of the resonon production. The

kinematical characteristics were simulated by means of combining two particles produced in the inelastic $\pi$-N or N-N collision into one resonon-particle:

$$M_{res}=\sqrt{E_{res}^2-P_{res}^2}\ ,\quad \vec{P}_{res}=\vec{P}_1+\vec{P}_2\ ,\quad E_{res}=E_1+E_2\ ,$$

where $\vec{P}_i$ and $E_i$ are momenta and energies of the particles. Despite a certain arbitrariness of such a procedure, after the resonon decay in every elementary act the correct multiplicity and correct angular and energy distributions of particles are preserved.

By combining various pairs of particles one can obtain not only the mesonic but the baryonic resonons, as well. As an estimate of characteristics of interactions of these resonons with nucleons one can take them to be equal to the corresponding characteristics of $\pi$-N and N-N interactions (for the same energy in the c.m.s.). The calculations performed indicate, however, that the account of resonons does not provide a saturation of the multiplicity $\bar{n}$ and excitation energy $E^*$; and a variation of these quantities turns out to be comparatively small (see Fig. 9). One cannot achieve the saturation even in the case when two resonons are assumed to be produced simultaneously in every inelastic $\pi$-N and N-N collision. The reason is that in the resonon production only the particles of first and second generations take part effectively, and their fraction with respect to the total number of particles in cascade shower is comparati-

vely small. Of course, this does not eliminate the fact that for some partial channels it is possible to point out such characteristics which will depend essentially on the resonon production.

4. By the present time a great deal of experimental data are stored for the fission of nuclei by the high-energy particles. However these data are very diverse and quite often agree bad with each other. In this situation it seems rather important to carry out fairly accurate and systematic calculations which then can be used as a basis for systematization of the experimental data. Divergences between theory and experiment which cannot be removed by a reasonable choice of parameters, could serve as starting point for a further improvement of the model. To this end we have performed a great amount of the Monte-Carlo calculations for high-energy nuclear fission. This cycle of calculations is based on the use of phenomenological approximation of the known experimental data on fission barriers from which "irregular part" due to shell effect , is singled out.

In order to pick out this part, the fission barrier was considered as a difference of the mass of nuclei in the saddle point and in the ground state: $B_f = M_{sp}(A,Z) - M(A,Z)$ (here and in the following $A$ is the mass number, $Z$ is the charge of the fissioning nucleus). In the first approximation for $M_{sp}$ one can neglect "shell correction" since the nucleus is very deformed in the saddle point, the

shell effect there should be considerably smaller than in the ground state. The shell correction $\Delta(A,Z)$ to the mass $M(A,Z)$ is taken from work by Cameron /9/ where it was determined as a difference between experimental value of the mass and that calculated according to liquid drop model. Besides, in order to obtain a better agreement between the ratio of fission-to-evaporation widths, which is defined as

$$\Gamma_n/\Gamma_f = \frac{4 m_n}{\pi \hbar^2} \frac{\int_0^{E-B_n} \varepsilon\, \sigma_{inv}(E,\varepsilon) \cdot \rho(E-B_n-\varepsilon)\, d\varepsilon}{\int_0^{E-B_f} \rho_{sp}(E-B_f-\varepsilon)\, d\varepsilon}, \quad (1)$$

$$\rho(E) = Const \cdot \exp 2\sqrt{aAE}, \quad \rho_{sp}(E) = Const \cdot \exp 2\sqrt{a_f AE}$$

( $a$ and $a_f$ are the parameters of level density of a nucleus for evaporation and fission) and the corresponding experimental data, some correction $\delta(A,Z)$ depending on an even-odd fissioning nucleus, proves to be necessarily introduced into the fission barrier

$$\delta(A,Z) = \begin{cases} +1 \text{ MeV, if } A-Z \text{ even} \\ -0.5 \text{ MeV, if } Z \text{ odd} \\ 0, \text{ otherwise} \end{cases} \quad (2)$$

(in fact this correction provides an account of a difference between pairing energies in the saddle point and in the ground state of a nucleus /10/).

From Fig. 10 it is seen that the regular part of fission barrier $B_f^0 = B_f^{exp} - \Delta(A,Z) + \delta(A,Z)$ turns out to be a rather

smooth function of the ratio $Z^2/A$, and it can be approximated by the expression

$$B_f^0 = 12.5 + \begin{cases} 4.7\,(33.5 - Z^2/A)^{3/4} \text{ MeV}, & \text{if } Z^2/A \leq 33.5 \\ -2.7\,(33.5 - Z^2/A)^{2/3} \text{ MeV}, & \text{if } Z^2/A > 33.5 \end{cases} \quad (3)$$

How well the ratio $\Gamma_n/\Gamma_f$ calculated by the formulae (1)-(3) agrees with experiment is shown in Fig. 11. The next figure demonstrates an excitation energy dependence of this ratio. Comparison of our values of $B_f$ and $\Gamma_n/\Gamma_f$ with results and approximations by other authors is given in Table 1.

A calculation of fission-evaporation competition for the excited residual nuclei which is based on the discussed above approximation of the barriers $B_f$ within the framework of the cascade theory involving the "trailing" effect, makes it possible to obtain a rather good agreement with experiment for fission cross sections $\sigma_f$ as well as for characteristics of accompanying particles throughout the whole energy region under investigation $T \simeq 0.05$–$30$ GeV (see Figs. 13,14)*.

Quite good agreement with experiment is achieved even for an yield of some isotopes, including the isotopes of which mass numbers are rather close to the mass number of initial nucleus (Fig.15).

Table II compares the excitation energies of fissioning

* It is of interest to note that at $T > 1$ GeV the fission cross section $\sigma_f$ decreases with increasing energy (see Fig. 13) if the decrease of nuclear density through the cascade development is not taken into account.

nuclei. From Fig. 16 it is seen that the distribution $W(E_f)$ has a long "tail" up to energies $E_f >> \bar{E}_f$, though the average excitation energy of fissionable nuclei $E_f$ is relatively small.

The calculated cross sections for fission of the nuclei Au, Bi, U by pions with energies T = 2.36 GeV: $\sigma_f$ = 122±17; 189±22; 780±72 mb are close to the experimental values taken from ref.[23]: $\sigma_f$ = 107±20; 191±40; 1090±160 mb accordingly.

Using the above approximation for fission barriers we have computed the excitation functions for heavy-ion reactions. The calculations rest on the Monte-Carlo variant of statistical description for a behaviour of highly excited nucleus with large angular momentum. This variant has been developed in work[11]. For heavy-ion reactions the calculation results (see Fig. 17) turn out to be more sensitive to the fission parameters. In particular, to obtain agreement with experiment, apparently it is necessary to assume, that the value of the level density parameter for the nuclei which deexcite by the evaporation, differs from that for fissioning nuclei ( $a \neq a_f$ ).

5. In connection with the obtaining of the relativistic nuclei beam in Dubna and Brookhaven, a development of models which describe inelastic collisions of high-energy nuclei with nuclei, is of particular interest at the present time.

It is clear from the very beginning that a calculation of such collisions is rather complicated problem not only in principle (because experimental information is negligible and many properties of the phenomenon remain still unclear), but also from the "calculation point" of view. Therefore it is reasonable to start with calculations of the most light nuclei: d, t, $^3$He, $^4$He.

Since a deuteron is very loosely bounded system, one can hope that the treatment of inelastic deuteron-nucleus collision as a superposition of two intranuclear cascades initiated by the deuteronic nucleons, will be a rather good approximation [12-14]. In such a consideration deuteron can be treated as a "dumb-bell" formed by a proton and a neutron, with fixed mean distance between them and with relative momentum given by the squarred Fourier transform of the deuteron wave function. In other respects our calculations follow exactly the cascade-evaporation model for nucleon-nuclear interactions. It is noteworthy that such a model takes into account naturally the stripping process.

Fig. 18 illustrates how well the theory agrees with experiment. As it is seen, this agreement is quite satisfactory. Just as in the pion- and nucleon-nucleus collisions, in the energy region $T \gtrsim 3$-5 GeV/nucl. the mean multiplicity of $h^-$ and $g$-prongs suffers "saturation"*.

*It should be emphasized that due to the trailing effect, the deuteron-nuclear interaction is not pure superposition of two independent nucleon-nuclear cascades.

Figure 19 shows the calculation results of intranuclear cascades for the interactions $t$ + nucleus, performed under the same assumptions as for the case of $d$ + nucleus. It is impossible to pass over a tendency to a decrease of energy at which the "saturation" of multiplicity of $h$- and $q$- prongs becomes noticeable.

6. As to the interactions with heavier incident nuclei, a possibility for direct use to them of the discussed simple model considering the reaction mechanism as a superposition of the cascades initiated by separate nucleons of the projectile is not so apparent. Therefore for the interactions $\alpha$+nucleus the more detailed theory has been worked out[15].

A motion of the fast $\alpha$-particle (as well as secondary nuclei $t$ and $^3He$ )inside a nucleus was regarded as a motion of the single system which can interact with any nucleon of the target-nucleus falling into a cylinder with radius $r_{int} = \rho + \lambda\!\!\!^{-}$ where $\lambda\!\!\!^{-}$ is the de Broglie wave-length of the $\alpha$ particle (or $t$ , $^3He$ ) and $\rho$ is of the order of the $\alpha$ -particle radius. It was assumed that the inelastic interaction of $\alpha$ -particle proceeds through the elastic or inelastic (with pion production)collision of intranuclear nucleon with one of the $\alpha$ -particle nucleons. Such N-N-collisions were computed just in the same fashion as in ordinary nucleon-nucleus cascade, but at the same time there were taken into account the Fermi motion of a target nucleon and the relative momentum of the nucleon inside $\alpha$ -particle. As to other three nucleons of the $\alpha$ -particle, these can

be emitted after the $\alpha$-$N$-interaction unbounded with each other or in the form of combinations $N+d$, $t$, $^3He$. Energies and emission angles for these particles are defined by the energy-momentum conservation law for the system composed by $\alpha$-particle and a nucleon of the target-nucleus. For probabilities of separate channels of the reaction the available experimental data were employed.

It should be noted that our model is more precise than those proposed in refs./6,7/, and is applicable at considerably higher energies $T$. However, in order to be able to compare various approaches, we have computed the $\alpha$-particle-nucleus collisions within the framework of a "simplified" model in which the $\alpha$-particle is regarded as four individual nucleons, each of them can initiate the intranuclear cascade.

As the comparison reveals, the present, not numerous and rather unaccurate experimental data can be agreed with both considered calculation variants. These data turn out to be not very sensitive to the details of the calculation (certainly, apart from an yield of fragments $t$, $^3He$; see Figs. 20-22).

7. An attempt to consider the interactions with the heavy ions using even the simplified variant of the cascade-evaporation model meets with serious difficulties unfortunately. A highly different approach was needed for calculations of such interactions. The basic lines of this approach are as follows:

a) Both nuclei are treated as they consist of separate nucleons the locations of centers $r_i$ of which are sampled

according to the experimental densities $\rho_1(r)$ and $\rho_2(r)$ under condition $|r_i - r_j| \geq \Delta$. Taking into consideration the diffusivity of the nuclear density and the potential it turns out to be very convenient to give up the division of nucleus into zones with the constant values of density $\rho(r)$. This is achieved by passing to the limit of the very large number of zones, what corresponds to the introduction of the radial dependence of the Fermi boundary-energy which is determined by the local nucleon density in accordance with the formulas for the degenerated Fermi-gas. (Legality of such procedure had been tested by means of the comparative calculations for the case of the nucleon-nucleus interactions).

b) The way of "decomposition" of the incident nucleus into A of its constituent nucleons is very important. It is mandatory that the condition

$$\sum_{i=1}^{A} T_i + A \cdot m_n = M = A m_n - \varepsilon A \quad \text{that is} \quad \sum_{i=1}^{A} T_i = -\varepsilon A ,$$

(where $m_n$ is the nucleon mass, $\varepsilon$ is the mean binding energy of the particle inside the nucleus) is fulfilled, if the kinetic energy $T_i$ of each of these nucleons is sampled in the c.m.s. of the incident nucleus. Sure this has no sense, the condition becomes quite reasonable: $\sum_{i=1}^{A} T_i' = \varepsilon A$ however, if the fact of the binding of the particle inside nucleus is taken into account by means of the change $m_n \to m_n' = m_n - \varepsilon$, $T_i \to T_i' = T_i + \varepsilon$.

Thus, we must sample out the value $T_i'$ of the Fermi distribution and, like handling the conventional nucleon-nucleus cascade[18], succeed in fulfilling the energy-momentum

conservation law for the nucleons of the primary in its own reference frame regarding these nucleons as having the mass $m'_n$. If one now passes over to the lab. reference frame, reverting to the mass $m_n$ and conserving total energy of the particle, then it is easy to convince ourselves that the energy conservation law will be fulfilled although the conservation law for the momenta of nucleons will be out of balance slightly.

The exact fulfilment of the energy conservation law permits to calculate correctly the excitation energy of the target nucleus. The excitation energy of the incident nucleus has been found from the energy of the "holes" left by the knocked out nucleons.

c) Every cascade nucleon can interact with each of the nucleons of the target nucleus the centre of which is located inside the cylinder with the radius $r_{int} = r_0 + \lambda\!\!\!^{-}$ ( $r_0 \simeq 1.3 \cdot 10^{-13}$ cm /6/) and the axis directed along the velocity vector of this nucleon. It is convenient here to trace the development of the cascade as depending on time. For this purpose at a moment $t$ the partners of the interaction are simulated for each cascade particles and the preference is given to that nucleon the time of which till the collision turns out to be minimal ( $t = \Delta t_{min}$). After this the state of the system (that is the location of all fast cascade particles) is recalculated to the moment $t + \Delta t$. If the nucleon of the target nucleus which underwent the interaction entered other cylinders as well and, consequently, could be the potential partner for the collision with other cascade

particles, then the partners of interaction at the moment $t + \Delta t$ for these cascade particles should be chosen anew, otherwise the partners remain the same.

d) The target nucleon which suffered the interaction further is considered as a cascade particle. This permits to take account of the local decrease of the nuclear matter density.

e) Each collision undergoes the test of the fulfilment of the Pauli principle with respect both to the target and to the incident nucleus.

f) The evaporation stage is calculated for each excited nucleus which is formed after passing the intranuclear cascade process. Moreover if the mass number of the residual nucleus $A \leq 4$ then the excitation is distributed equally among the nucleons of this nucleus.

The remaining details of the calculations are the same as for the cases of pion- and nucleon-nucleus collisions.

The method considered has been tested in the case of the nitrogen-ions-$^{70}$Ga-nuclei interactions for T = 0.2;0.4 and 7 GeV/nucleon. The obtained results (preliminary for the present) can be compared with the photoemulsion data for the interactions of the cosmic nuclei (of the M group basically) in the energy range of T=0.1-0.3, 0.3-0.5 and 2-15GeV/nucl. /19,21/

As can be seen from Table III and Fig. 23 the experimental and theoretical values of the mean multiplicity of the secondary particles and their distributions are pretty close

each other, this is especially so if one recalls that in experiment there is distribution with respect both to the energy and composition of the initial nuclei and to the composition of the target nuclei. Besides several quantities ( $\bar{n}_{\pi}$ for example) in the works[19,21] were not measured directly but have been obtained by means of recalculation on the basis of some assumptions.

However it should be noted some excess exceeding the experimental uncertainties of the calculated multiplicity of b- and g-particles over the experimental one, especially for the case of T = 7 GeV/nucleon. This witnesses some overestimating of the number of the intranuclear collisions.

The fact that the nucleons of the incident nucleus must pass through the target nucleus with smaller number of interactions manifests itself in the angular distributions of particles, as well. It can be seen from fig. 24 that the noticeable divergence in the angular distributions of the g-particles at the angles $\theta \lesssim 40°$ and $\theta \lesssim 30°$ at T=0.2 and 0.4 GeV/nucleon takes place. These are just values of $\theta$, which correspond to the kinematical limit for particles emitted from the incident nucleus. The model gives too small number of such nucleons. When going to the energy T=7 GeV/nucl. one observes that the "passing through" nucleons and particles evaporated from the primary will contribute to the s-particles already and that the agreement between the experimental and theoretical angular distributions for the g-particles becomes very good.

In Fig. 25 the energy distributions of protons are shown. One can note here the quite satisfactory agreement between experiment and theory.

* * *

Hence, during the last years the significant progress can be noted in the development of the Monte-Carlo cascade-evaporation theory of the nuclear reactions. Nowadays this theory, when taking account of the processes of fission, permits to calculate rather effectively very broad scope of phenomena concerning the inelastic interactions of particles and nuclei with nuclei. At the same time the theory is far from having exhausted its possibilities and it can be improved significantly first of all for the applications to the calculation of the interactions of the relativistic nuclei and for the taking account of the nonstationary decay processes (for the interactions with the light nuclei especially).

Further progress of the theory highly depends on the storage of sufficiently accurate and, mainly, of sufficiently complete experimental data.

## References


1. V.S.Barashenkov, K.K.Gudima, A.S.Iljinov, V.D.Toneev. Communication of JINR P2-5118, Dubna, 1970.
2. V.S.Barashenkov, A.S.Iljinov, N.M.Sobolevskii, V.D.Toneev. Communication of JINR J2-5549, Dubna, 1970.
3. V.S.Barashenkov, A.S.Iljinov, N.M.Sobolevskii, V.D.Toneev. Communication of JINR E2-5813, Dunba,1971.
4. V.S.Barashenkov, V.D.Toneev. "Interactions of High Energy Particles and Nuclei with Nuclei .", M.,Atomizdat,1972.
5. V.S.Barashenkov, H.W.Bertini, K.Chen, G.Friedlander, G.D.Harp, A.S.Iljinov, J.M.Miller, V.D.Toneev; BNL-16429, 1971.
6. V.S.Barashenkov, A.S.Iljinov, V.D.Toneev. Jad.fiz. 13,743 (1971).
7. V.S.Barashenkov, A.S.Iljinov, V.D.Toneev. Communication of JINR E2-5282, Dubna, 1970.
8. A.S.Iljinov, V.D.Toneev. Communication of JINR P2-5546, Dubna, 1971.
9. A.G.W.Cameron, Canad. J.Phys. 35, 1021 (1957).
10. L.G.Moretto, R.C.Gatti, S.G.Thompson, J.R.Huizenga, J.O.Rasmussen. Phys.Rev. 179, 1845 (1969).
11. A.S.Iljinov, V.D.Toneev. Jad.fiz. 9, 48 (1969),
12. V.S.Barashenkov, K.K.Gudima, V.D.Toneev. Jad.fiz.9,528 (1969), 10, 760 (1960).
13. K.K.Gidima, A.D.Kirillov, V.D.Toneev, Ju.P.Jakovlev. Communication of JINR P2-5261, Dubna, 1970.
14. V.S.Barashenkov, A.S.Iljinov, V.D.Toneev. Communication of JINR P2-5548, Dubna, 1971.
15. V.S.Barashenkov, K.K.Gudima, F.G.Gereghi, A.S.Iljinov, V.D.Toneev. Communication of JINR P2-6195,Dubna,1971.

16. A.I.Vihrov, V.E.Dudkin, I.I.Pjanov, O.V.Sysoeva. Jad.fiz. II, 36 (1970).

17. T.A.Gabriel, R.T. Santoro, R.G.Alsmiller; Nucl.Sci . and Eng. 44, 104 (1971).

18. V.S.Barashenkov, K.K.Gudima, V.D.Toneev. Acta Phys.Polonica 36, 415 (1969).

19. B.Anderson, I.Otterlund, K.Kristianssen; Ark.Fys. 31,527 (1966).

20. I.Otterlund; Ark.Fys. 38, 467 (1968).

21. I.Otterlund, R.Resman; Ark.Fys. 39, 265 (1969).

22. R.Resman, I.Otterlund; Physica Scripta 6, 183 (1971).

23. L.Husain, S.Katcoff. Phys.Rev. 46, 263 (1971).

Table 1.

Fission barriers and ratio of widths $\Gamma_f/\Gamma_n$ for various uranium isotopes

| Mass number of fissioning nucleus | $B_f$, Mev | | | $\Gamma_f/\Gamma_n$ | | |
|---|---|---|---|---|---|---|
| | Theory | | Experiment b) | Theory | | Experiment[d] |
| | the present work | Myers, Swiatecki[a] | | the present work ($E^*$=10Mev) | Sikkeland[c] | |
| 230 | 5,68 | 4,655 | - | 0,27 | 0,25 | - |
| 231 | 4,05 | 4,724 | - | 0,46 | 0,34 | - |
| 232 | 6,00 | 4,798 | - | 0,46 | 0,47 | - |
| 233 | 4,65 | 4,873 | 5,49 | 0,76 | 0,64 | I,0 |
| 234 | 6,54 | 4,950 | 5,25 | I,I0 | 0,89 | 0,85; I,6 |
| 235 | 5,I4 | 5,027 | 5,78 | I,66 | I,2 | I,2; I,6 |
| 236 | 6,97 | 5,I05 | 5,44 | 2,42 | I,7 | I,6; 2,I |
| 237 | 5,59 | 5,I84 | 6,40 | 3,24 | 2,3 | 3,0 |
| 238 | 7,25 | 5,262 | 5,7 | 5,23 | 3,2 | 4,0 |
| 239 | 5,80 | 5,340 | 6,20 | 5,75 | 5,I | 4,5 |
| 240 | 7,47 | 5,4I8 | - | 8,60 | 6,I | - |

a) W.D.Myers, W.J.Swiatecki; Nucl.Phys.81,1(1966); Berkeley Report UCRL-11980,1965.
b) Experimental data are taken from R.W.Hasse.Ann.Phys.68, 377 (1971).
c) T.Sikkeland; Phys.Rev. 169, 1800 (1968).
d) R.Vandenbosh, J.R.Huizenga; Paper P/1688 Proceedings of the Second United Nations Conference on the Peaceful Uses of Atomic Energy, 15, Geneva, 1958.

Table 2

Average excitation energies (after the cascade stage) for the fissinable nuclei produced in interactions of protons of energy T with uranium

| T Mev | I40 | 340 | 460 | 660 |
|---|---|---|---|---|
| Experiment[a] | 80±20 | I40±40 | I65±45 | I85±60 |
| Calculation results | 68±7 | 90±8 | I38±I4 | I59±I6 |

a) V.P.Shamov; Dokl. AN SSSR, 103, 593 (1953).

Table 3.

Average multiplicity of particles produced in inelastic collisions of the nitrogen ions with photoemulsion nuclei

| | T = 0,2 Gev/nucleon | | T = 0,4 Gev/nucleon | | T = 7 Gev/nucleon | |
|---|---|---|---|---|---|---|
| | Theory | Experiment /21,22/ | Theory | Experiment /21,22/ | Theory | Experiment /19,21/ |
| $\bar{n}_s$ | I,9±0,2[a] | I,48±0,22[a] | I,9±0,2[a] | 2,20±0,30 | I3,I±I,2 (8,9±0,8)[b] | I4,8±2,3 (I2,I±I,I)[b] |
| $\bar{n}_g$ | 4,0±0,3 | 4,I4±0,37 | 6,7±0,6 | 6,78±0,53 | 8,2±0,7 | 6,0±0,7 |
| $\bar{n}_g$ | 3,4±0,3 | 3,I4±0,32 | 4,4±0,4 | 5,04±0,46 | 7,I±0,6 | 5,3±0,6 |

a) The number of sparse-black prongs is indicated ($30 < \mathcal{J} < 100$ Mev)

b) In parenthesis the average number of pions is presented.

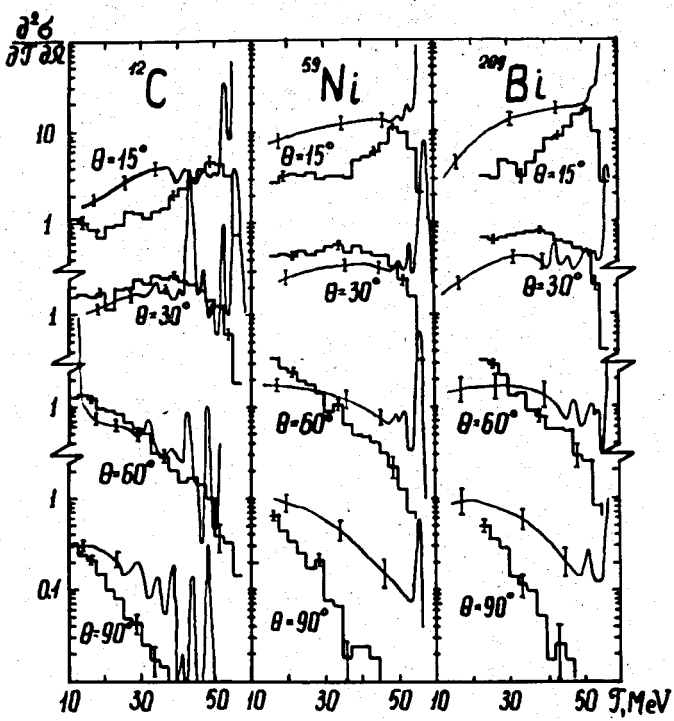


Fig. 1. Energy spectra of the protons emitted at the angle $\theta$ from various nuclei irradiated by the proton beam of energy T=57 MeV (in mb/MeV·steradian). The histograms are the calculation results, the experimental data are taken from work of Monaka et al. (J.Phys.Soc.Japan 47,1817 (1962)).

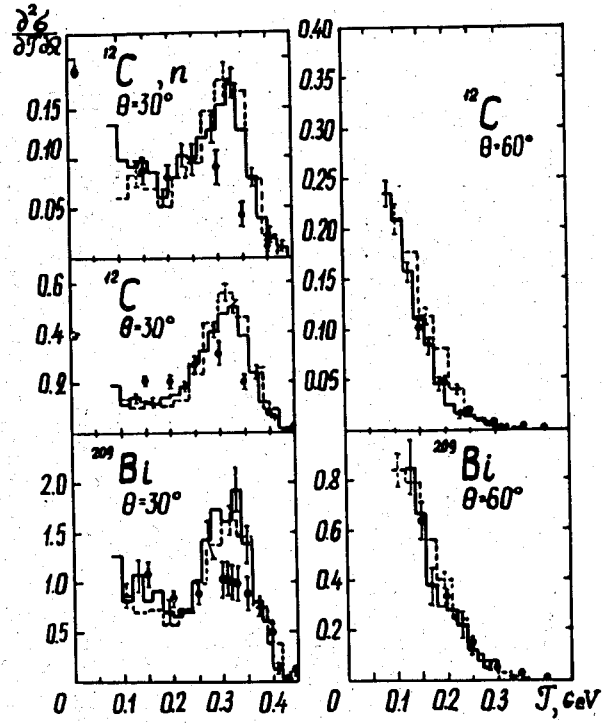


Fig. 2. Energy spectra of the protons and neutrons (the left upper Fig. ) emitted from the nuclei of carbon and vismuth bombarded by the primary protons of energy T=450 MeV (in mb/MeV·steradian). The solid histograms present our results and the dashed ones are Bertini results (Phys.Rev. 188,1711(1969)). Experimental data are taken from work of Wachter et al. (ORNL-TM-2253,1968).

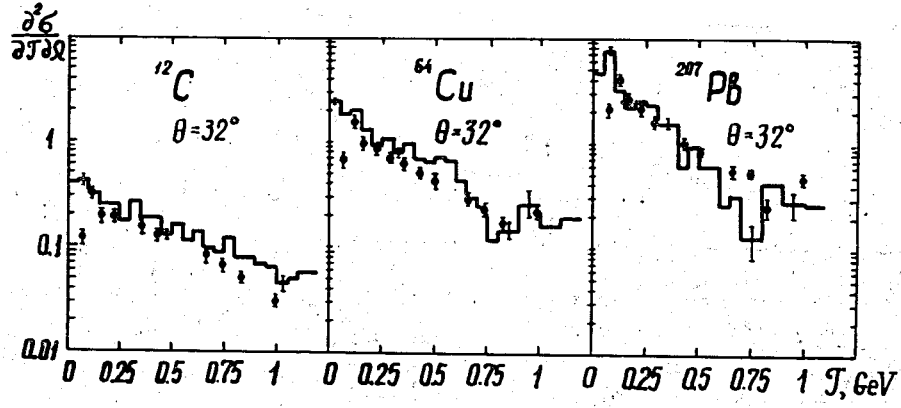


Fig. 3. Energy spectra of the protons emitted by different nuclei bombarded by the primary protons of energy T=3 GeV (in mb/MeV·steradian). The histograms are calculations, the experimental points are taken from work of Edge et al. (Phys.Rev. 183, 849 (1969)).

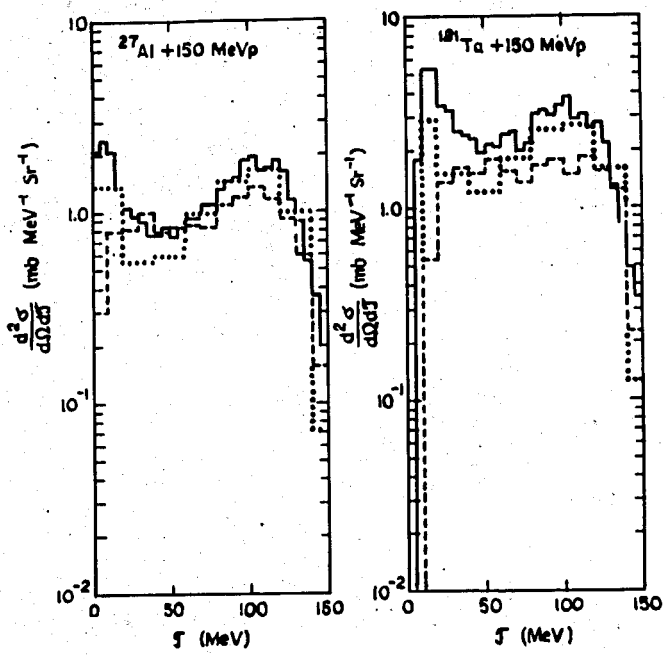


Fig. 4. Energy spectra of emitted protons at $\theta = 25^{\circ} - 35^{\circ}$. The solid, dashed and dotted histograms are the results obtained from the JINR, Brookhaven and Oak-Ridge models, respectively.

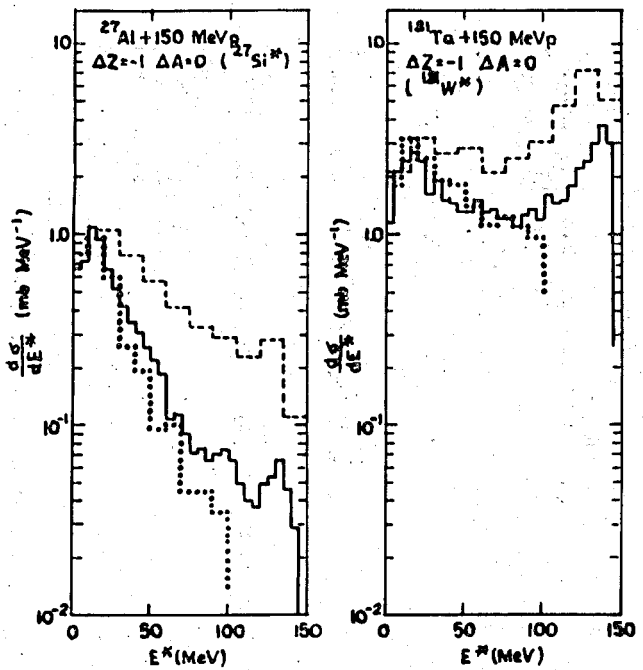


Fig. 5. Excitation energy distributions for cascade product nuclei produced in (p, N) reactions.
Notations are the same as in Fig. 4.

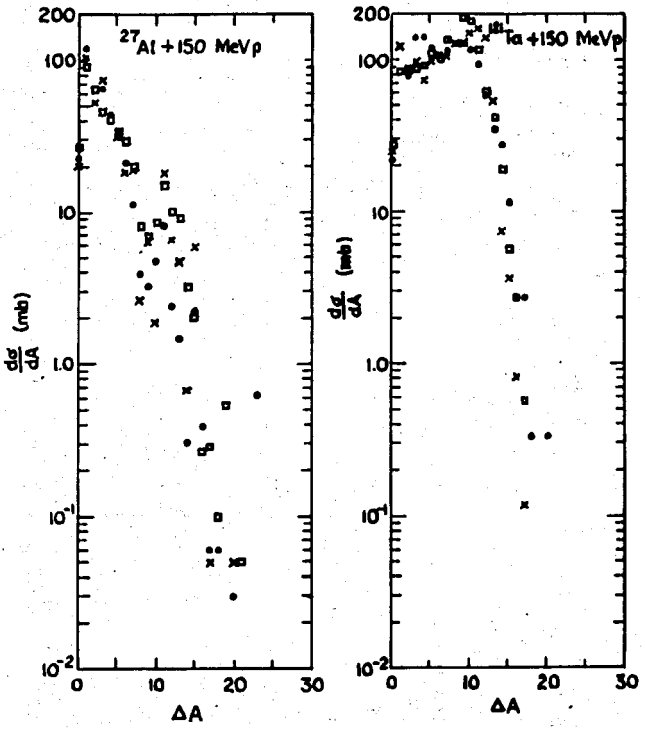


Fig. 6. Mass yields. The dots, squares and crosses are the results obtained from the JINR, Brookhaven and Oak-Ridge models, respectively.

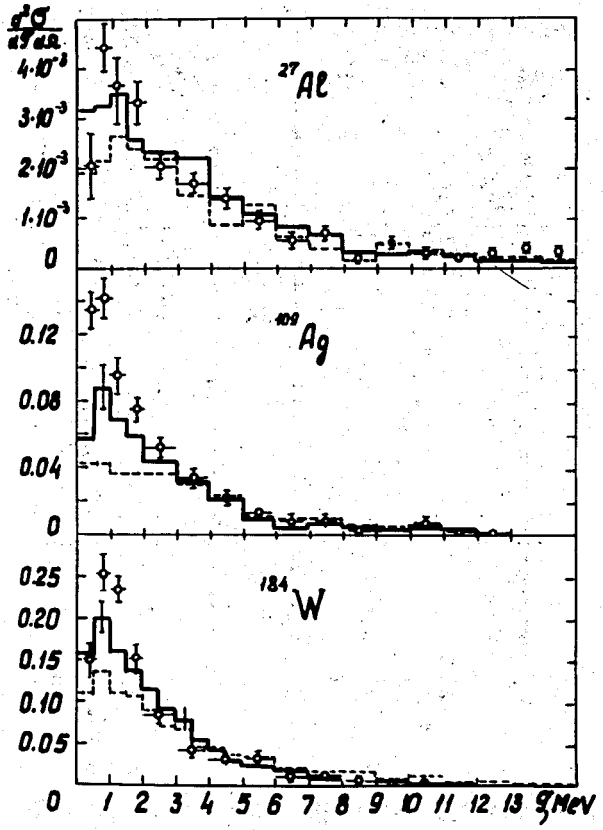


Fig. 7. Energy spectra of evaporation neutrons emitted at the angle $\Theta=180°$ from nuclei $^{27}Al$ irradiated by 150 MeV protons. Solid and dashed histograms are the calculations for the level density parameter $a=A/10$ and $a=A/20$ $MeV^{-1}$, respectively. For the bibliography on the experimental data see Ref./4/.

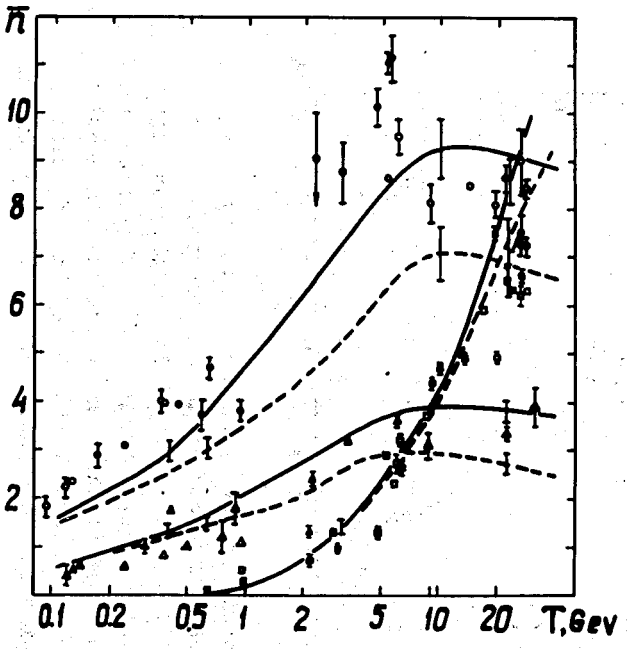


Fig. 8. Energy dependence of the average multiplicity of s-, g- and h- particles produced in photoemulsion by the protons of energy T. These results have been obtained taking into account the "trailing" effect. The dashed line is the calculations under the condition $n_h > 1$. The marks o, $\Delta$ and $\square$ are the experimental values of $\bar{n}_h$, $\bar{n}_g$ and $\bar{n}_s$, respectively, obtained by scanning "along track", the shaded marks relate to the values obtained by scanning "over the area".

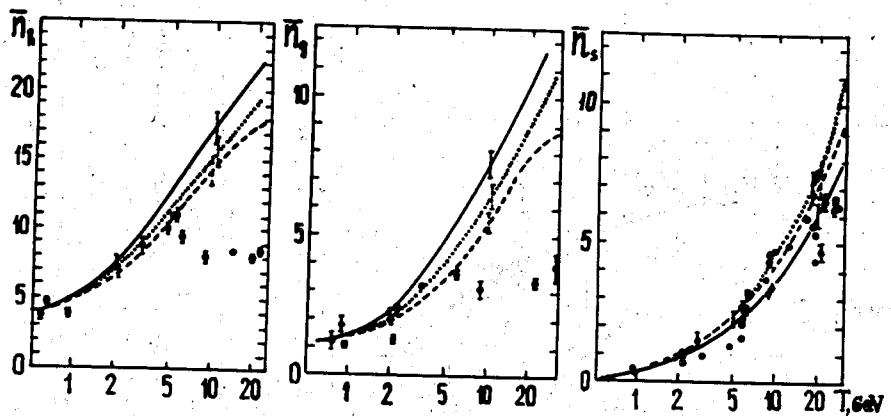


Fig. 9. Energy dependence of the average multiplicity of s-, g- and h- prongs produced in the interactions of protons with emulsion nuclei. The solid, dashed and dotted curves denote, respectively, the calculations by means of the conventional cascade-evaporation model (without the "trailing effect") and of the variants with production in every inelastic collision of one or two resonons. For comparison the experimental data are presented as well.

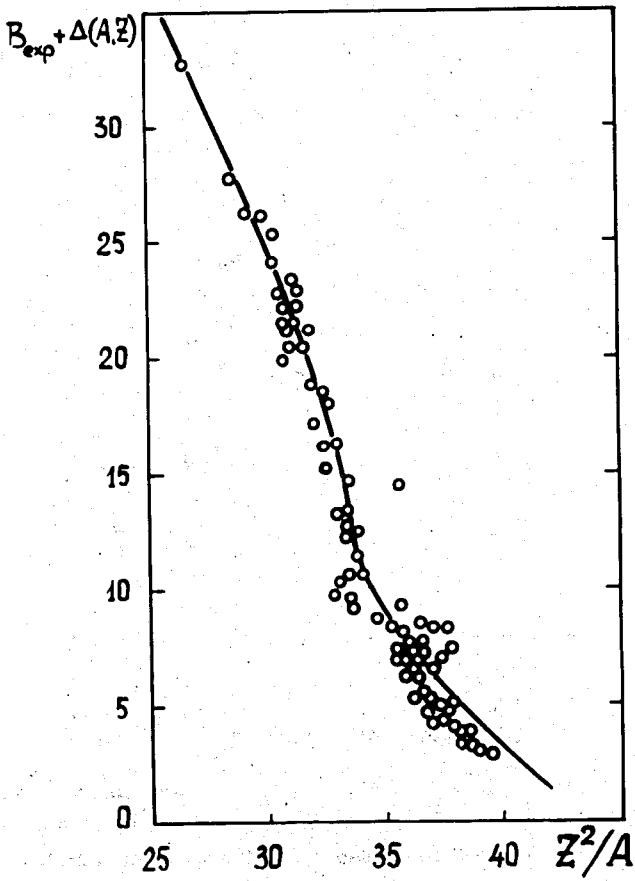


Fig. 10. Comparison with calculated of the experimental values for the fission barrier. The curve is the calculation by the formula (3).

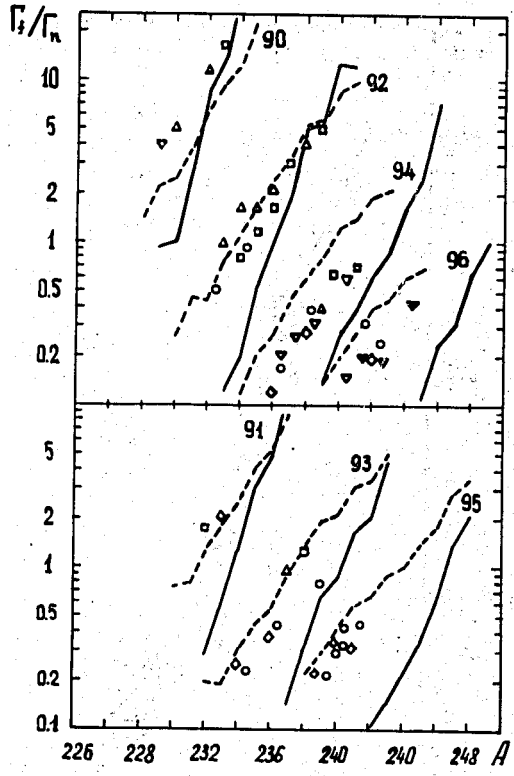


Fig. 11. Dependence of the ratio $\Gamma_n / \Gamma_f$ on the mass number and charge of fissioning nucleus. The solid and dashed lines denote calculation results for the excitation energy $E^*$=10 and 20 Mev, respectively. The upper figure relates to even Z, the lower figure to odd Z. Experimental data are taken from work of Vandenbosh and Huizenga. (Paper P/1688 Proceedings of the Second United Nations Conference on the Peaceful Uses of Atomic Energy, 15, Geneva, 1958).

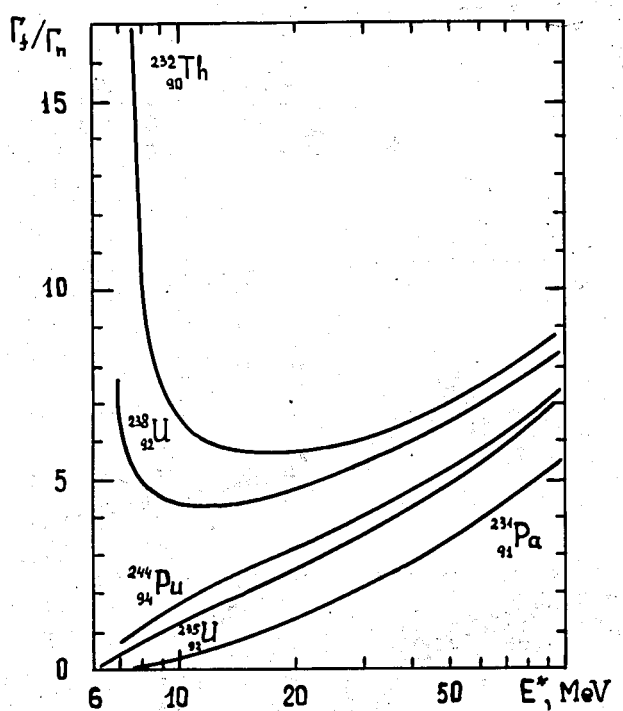


Fig. 12. The ratio of neutron-evaporation-to-fission widths $\Gamma_n/\Gamma_f$ depending on value of the nucleus excitation energy E*. The experimental points are taken from the previous figure.

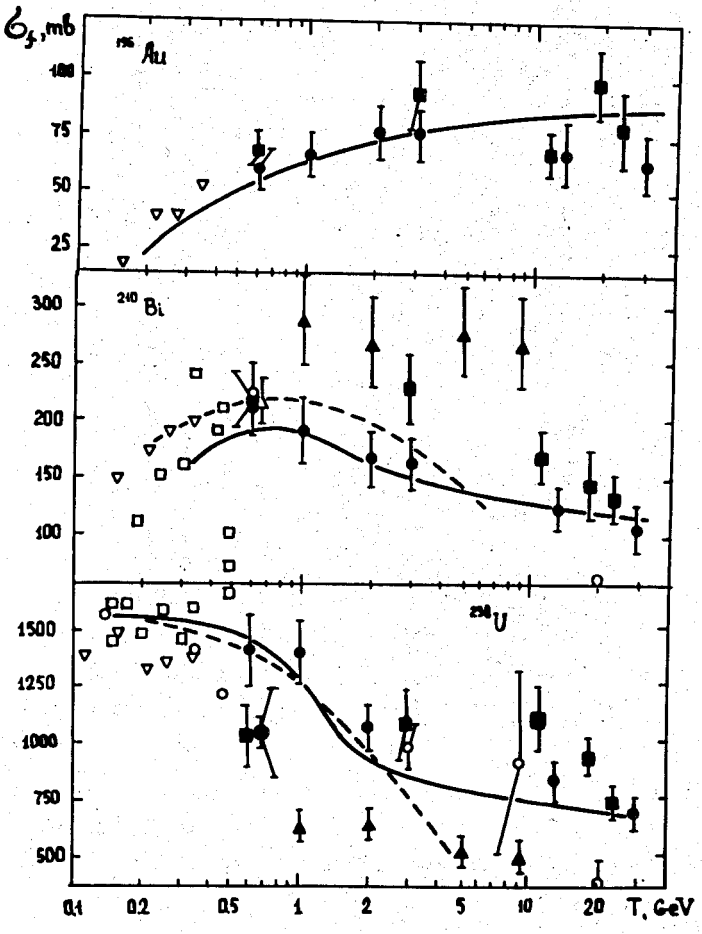


Fig. 13. The fission cross sections by protons of energy T. The solid and dashed curves are the calculation results involving and without involving the "trailing" effect, respectively.

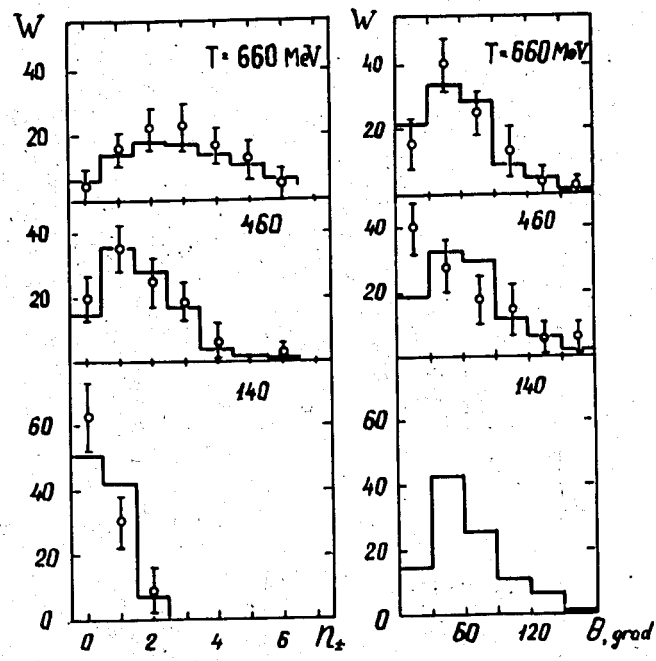


Fig. 14. Distributions of charged particles over the multiplicity and emission angles for $p + {}^{238}U$ collisions followed by fission. The histograms are the calculation results. Experimental data are taken from work of Ivanova and P'janov (ЖЭТФ 31, 416 (1956)). The primary proton energy T is indicated.

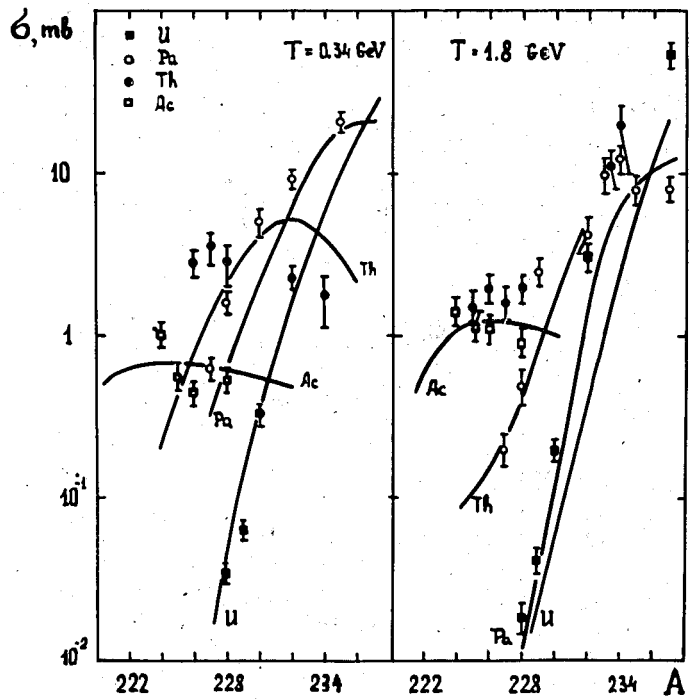


Fig. 15. Yield of various isotopes at irradiating of nuclei by the protons of energy T=0.34 and 1.8 GeV. Experimental data are taken from work of Lindner and Osborn (Phys.Rev. 103, 378 (1956)) and of Pate and Poskanzer (Phys.Rev. 123, 647 (1961)).

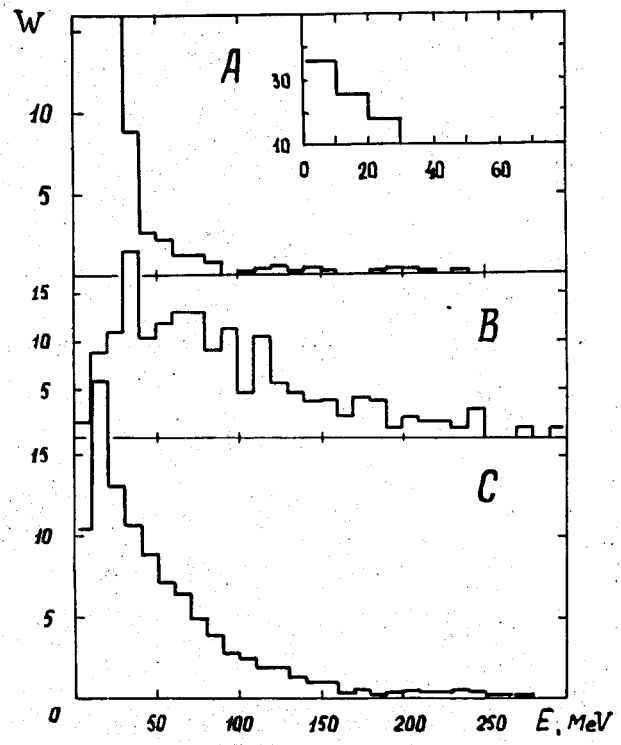


Fig. 16. Excitation energy distribution for nuclei produced in $p + {}^{238}U$ interactions at $T = 340$ MeV. A is the distribution for events without fission, B is the energy distribution for fissioning nuclei after the cascade development and C is the energy distribution of the fissioning nuclei just before their fission.

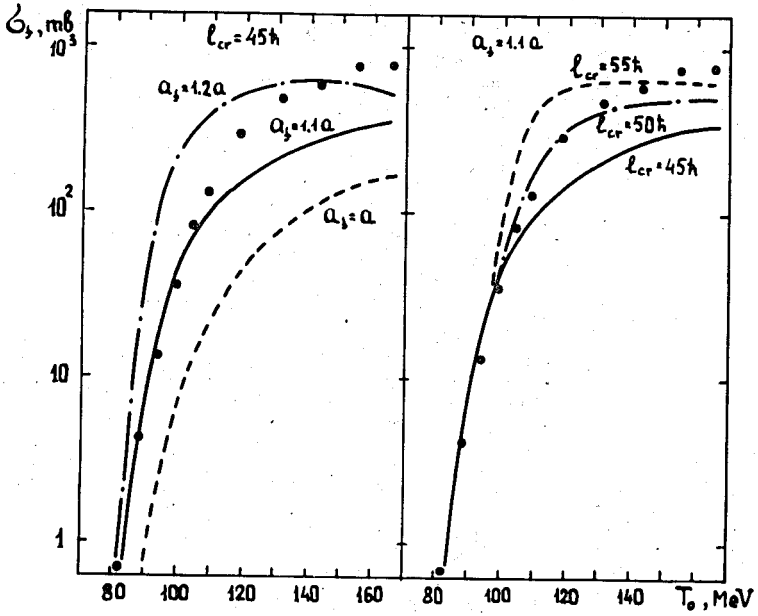


Fig. 17. The fission cross sections of $^{174}Yb$ nuclei by $^{16}O$ ions with energy T. The curves are the calculation results for various values of the critical angular momentum $\ell_{cr}$ and for different choice for value of the level density parameters $a$ and $a_f$. Experimental points are from work of Sikkeland (Phys.Rev. 135,669B (1964)).

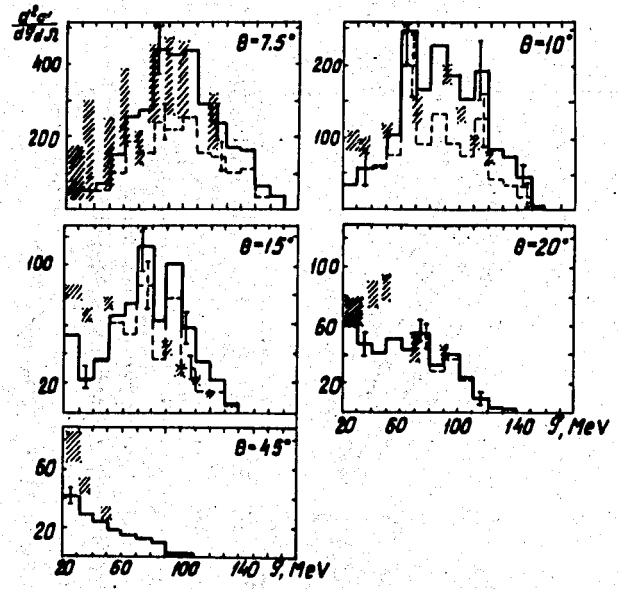


Fig. 18. Energy spectra of protons produced in inelastic $d + {}^{238}U$ collisions at T=95 MeV/nucl. The solid histogram is the calculation resultsfor the diffusive nucleus, the dashed histogram is the calculation results obtained in the approximation by sharp boundary of a nucleus without diffractive and Coulomb splittings. The shaded areas denote the experimental data errors of Milburn et al. (Phys.Rev. 95,1268 (1954)).

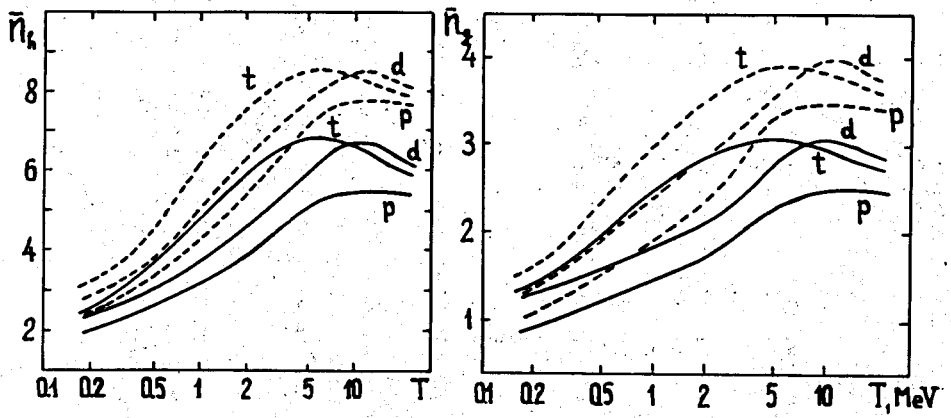


Fig. 19. The average multiplicity of $g$- and $h$-prongs in emulsion stars produced by protons and light nuclei $d$ and $t$. The dashed curves relate to the stars with an auxiliary selection criterion $n_h > 1$.

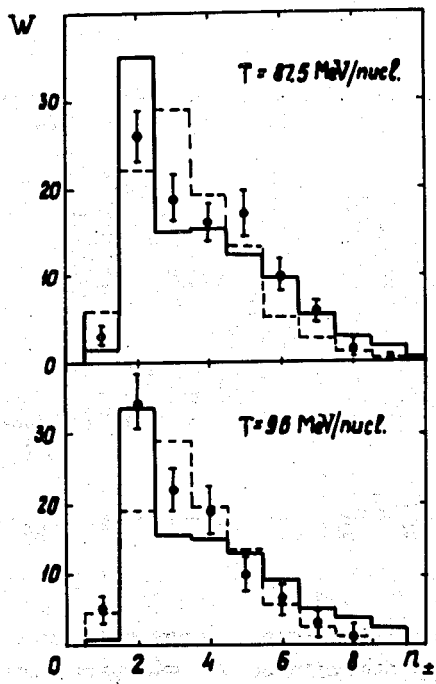


Fig. 20. Distributions of prongs in emulsion stars produced by $\alpha$-particles of energy T. Experimental points are taken from work of Quareni and Zorn (Nuovo Cim. 1, 1282 (1955)) and Willonghby (Phys.Rev. 101, 324 (1956)). The histograms are the calculation results, the dashed line presents the results obtained from the "simplified" model.

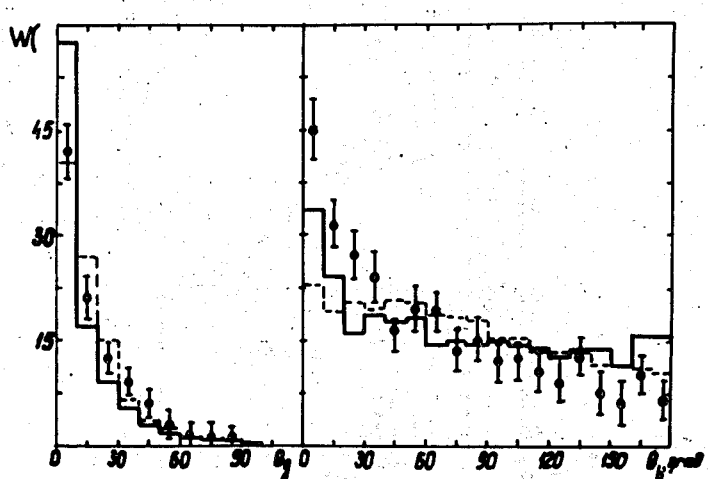


Fig. 21. Angular distributions of grey and black tracks produced in photoemulsion by $\alpha$-particles of energy T = 95 MeV/nucl. Experimental data are taken from work of Willoughby (Phys.Rev. 101, 324 (1956)). All notations are the same as in Fig. 20.

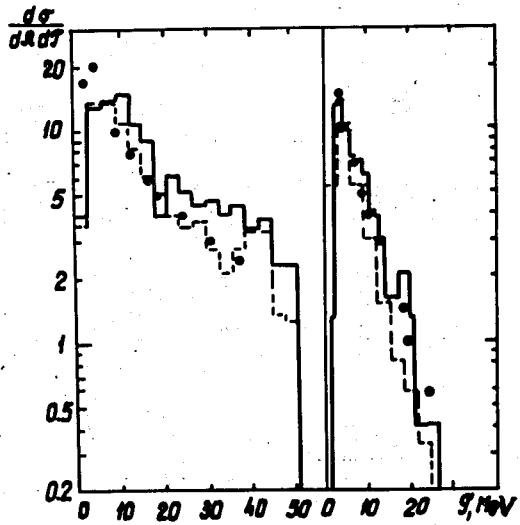


Fig. 22. Energy spectra of the protons emitted at the angle θ from the nuclei $^{27}Al$ irradiated by $\alpha$-particles of energy T=51 MeV/nucleon (in mb/MeV·steradian). The experimental points are taken from work of Baily (UCRL-3334, 1956). Notations are the same as in Fig. 20.

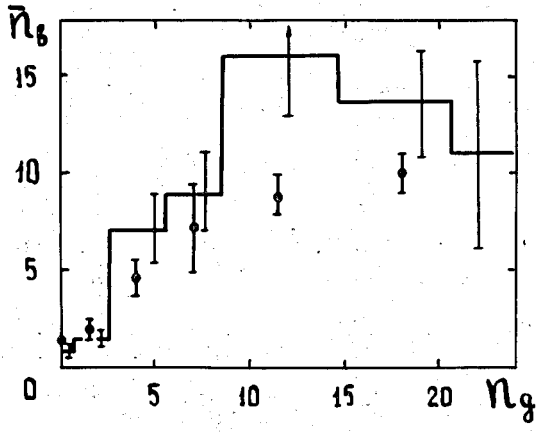


Fig. 23. Correlations $\bar{n}_b = f(n_g)$ in photoemulsion stars produced by $^{14}N$ ions of energy T=7 GeV/nucl. The experimental points are taken from work /20/.

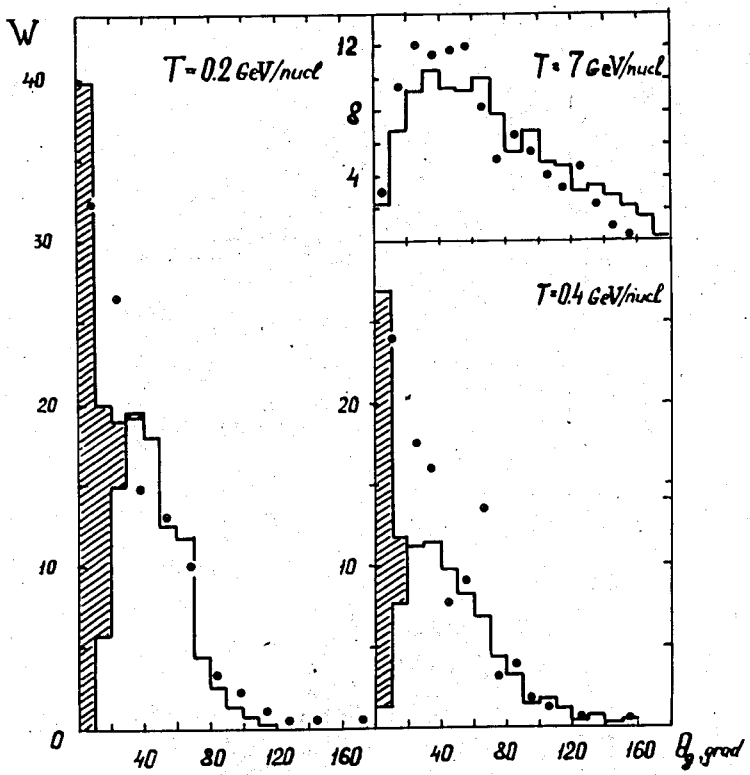


Fig. 24. Angular distributions of the grey prongs in emulsion stars produced by the nitrogen ions of energy T. The shaded areas denote the contribution of particles emitted from an incident nucleus. The experimental points are taken from Refs./19,22/.

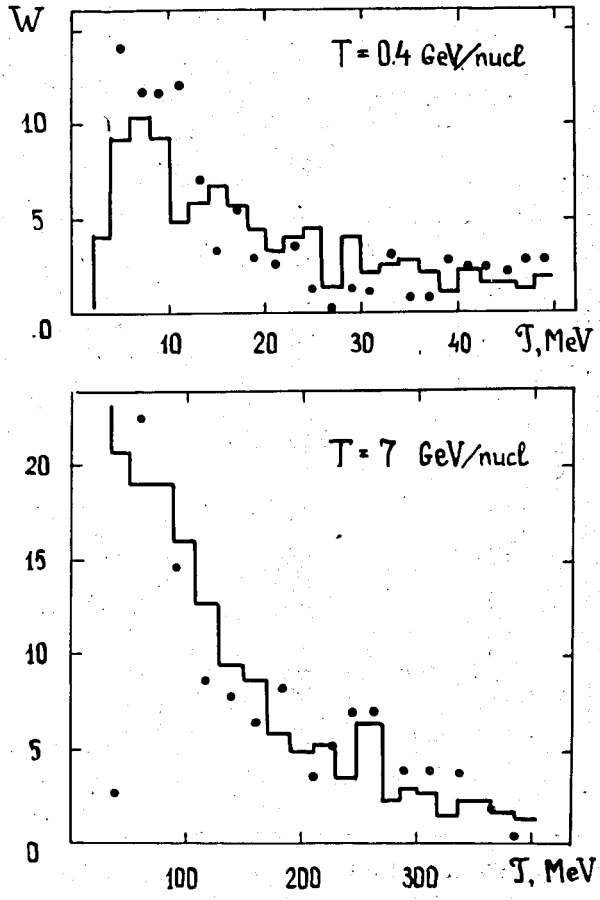


Fig. 25. Energy distributions of particles produced in interactions of the nitrogen ions of energy T with the emulsion nuclei. The experimental data are from Refs.[19,22].